

First-principles calculations of the magnetism of Fe₂O₂H₂

Sergey Stolbov,^{1,*} Richard A. Klemm,^{1,†} and Talat S. Rahman^{1,‡}

¹*Department of Physics, Kansas State University, Manhattan, KS 66506 USA*

(Dated: February 2, 2008)

By expanding the wave function in plane waves, we use the pseudopotential method of density functional theory within the generalized gradient approximation to calculate the effective magnetic coupling energies of the $S = 5/2$ spins in the Fe2 dimer, approximated as Fe₂O₂H₂. Setting the Fe-O bond length at the value corresponding to the minimum total energy, we find the difference in antiferromagnetic and ferromagnetic exchange energies as a function of the Fe-O-Fe bond angle θ . The effective interaction is antiferromagnetic for $63^\circ < \theta < 105^\circ$, and is ferromagnetic otherwise. Full potential augmented plane wave calculations were also performed at $\theta = 100, 105^\circ$, confirming these results, and providing information relevant to the local anisotropy of the spin interactions.

PACS numbers: 71.15.Mb, 61.46.+w, 75.75.+a

Single molecule magnets (SMM's) have been under intense study recently, due to their potential uses in magnetic storage and quantum computing.^{1,2,3} The materials consist of insulating crystalline arrays of identical SMM's 1-3 nm in size, each containing two or more magnetic ions. Since the magnetic ions in each SMM are surrounded by non-magnetic ligands, the intermolecular magnetic interactions are usually negligible. Although the most commonly studied SMM's are the high-spin Mn₁₂ and Fe₈,^{1,4} such SMM's contain a variety of ferromagnetic (FM) and antiferromagnetic (AFM) intramolecular interactions, rendering unique fits to a variety of experiments difficult.⁵

In many single molecule magnets, and in Fe₈ in particular, the magnetic core contains [LM(OR)]₂⁺ dimer ions,⁴ where M denotes a magnetic ion (eg. Fe³⁺), L is a ligand, and OR denotes an alkoxide ion, with R = H, CH₃, CH₂CH₃, etc. In Fe₈, the overall magnetic cluster is {[(tacn)₆Fe₈O₂(OH)₁₂]Br₇·H₂O}[Br·8H₂O], where tacn is 1,4,7-triazacyclononane.⁶ Near-neighbor Fe³⁺ ions are coupled via superexchange in four distinct pair bondings: four equivalent pairs of Fe³⁺ ions are coupled through two (OH)⁻ ions with Fe-O-Fe angle $\theta = 100.7^\circ$, one central pair is coupled via two O²⁻ ions with Fe-O-Fe angle $\theta = 104.4^\circ$, and each of those Fe³⁺ ions is coupled via the same O²⁻ ions to two other Fe³⁺ ions, and finally, four equivalent pairings via a single (OH)⁻ ion.^{6,7} Here we focus upon the magnetic superexchange interaction between the constituent magnetic ions that is mediated via two oxygen ions, which is different than the usual case of superexchange via a single oxygen ion. The attachment of alkyl R groups to the oxygen ions is probably of minor importance, because the oxygen orbitals involved in the OR bond are orthogonal to those involved in the Fe-O bonding. The local magnetic order depends strongly upon the Fe-O-Fe bond angle θ and the bond length, which are determined by the local ligand environment.

In addition, Le Gall *et al.* synthesized and measured the magnetization of four species of the isolated dimer Fe₂,⁸ and electron paramagnetic resonance (EPR) experiments were performed on one of them.⁹ These dimers

have the general formula [Fe(OR)(dK)₂]₂, where dK is a β -diketonate ligand. In these dimers, the oxygen ion in each alkoxide group forms a bridge between the Fe³⁺ S=5/2 spins, allowing them to interact via superexchange through both O²⁻ ions, as in the [LFe(OH)]₂²⁺ ions present in Fe₈. From magnetic susceptibility measurements, fits to the isotropic Heisenberg exchange model $\mathcal{H} = -JS_1 \cdot S_2$ were made.⁸ Note that we use the sign convention in which a positive J corresponds to ferromagnetic couplings. In comparing these four Fe2 dimers, they found no correlation between J and the average Fe-O bridging bond distance, but a linear correlation was found between J and the Fe-O-Fe bond angle θ , with J decreasing monotonically from -14.8 ± 0.5 to -19.0 ± 0.6 cm⁻¹ as θ increased from 101.8° to 103.8° , respectively.⁸ One of these compounds, [Fe(OMe)(dpm)₂]₂, was studied with Mössbauer spectroscopy.¹⁰

Le Gall *et al.* also compared these trends with predictions based upon extended Hückel calculations performed on the simpler model system, [Fe(OH)H₄]₂,⁸ using the approach of Hay, Thibeault, and Hoffman that for magnetic dimers, $J \propto \sum_i (\Delta E_i)^2$, where ΔE_i is the energy separation between symmetric and asymmetric combinations of coupled magnetic orbitals.¹¹ Unfortunately, when they used the oxygen orbital parameters normally expected, the J values calculated in this way increased with increasing θ , opposite to the experimental observations.⁸ That approach was also not applicable for ferromagnetic exchange couplings.¹¹

The static and dynamic properties of Fe2 dimers were studied theoretically by Efremov and Klemm, and interesting low temperature quantum steps in the magnetization were predicted.¹² Recently, those authors studied local spin anisotropy effects, and found that the details of the low temperature quantum magnetization steps could be complicated by such local anisotropies.¹³

Because of the very weak antiferromagnetic interactions ($J \approx -0.9 \pm 0.1$ meV) between the Fe(III) spins in the two related dimer compounds,^{14,15,16,17,18} μ -oxalatotetrakis(acetylacetonato)Fe₂ and [Fe(salen)Cl]₂, where salen is *N,N'*-ethylenebis(salicylideneiminato), magnetization steps were observed at low temperatures

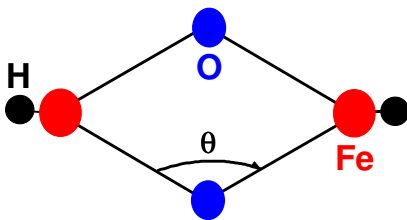


FIG. 1: Sketch of the $[HFeO]_2$ dimer. The Fe-O-Fe angle is denoted θ .

in them.^{19,20} In the former case, all five of the magnetization steps were observed using pulsed magnetic fields,¹⁹ and they were found to be evenly spaced, suggestive of an isotropic antiferromagnetic Heisenberg exchange interaction.¹² In the second case, the lower two and part of the third magnetization steps were observed by pulsed magnetic fields at low temperature. Although the second step was rather sharp, with a sharp dM/dH peak, the first step had a much broader linewidth, suggestive of two primary constituents.²⁰ Although the sample measured contained many unoriented crystallites, the broad first peak followed by the sharp second peak is consistent with a substantial amount of local spin anisotropy of the type $-J_a \sum_{i=1}^2 S_{iz}^2$, where $J_a \approx 0.1 J$.¹³

Here we focus on the constituent dimers present in Fe8, which are of the $[RFeO]_2$ type, in which each Fe^{3+} ion shares electrons with one aliphatic R group and two bridging O^{2-} ions, which have no aliphatic substitutions on them, as pictured for $R = H$ in Fig. 1. We model this system by replacing the R group with H. To study the geometry effect upon the magnetic interaction and the spin state of the dimer, we perform a first principles calculation of the electronic and magnetic structures and of the total energy of the $[HFeO]_2$ dimers for ferromagnetic and antiferromagnetic states and for $57^\circ \leq \theta \leq 110^\circ$. From these results, we are able to obtain $J(\theta)$.

The majority of the calculations presented here were performed within the density functional theory, using the generalized gradient approximation (GGA) for the exchange-correlation functional,²¹ and the pseudopotential method combined with the expansion of the wave functions in plane waves.²² We assume a three-dimensional structure of such $[HFeO]_2$ dimers, and for simplicity, pack them into a periodic array of tetragonal unit supercells of dimension $12 \times 12 \times 15 \text{ \AA}$. This unit supercell is sufficiently large that the interaction between neighboring dimers is utterly negligible. For all atoms in the dimer, we use the ultrasoft pseudopotentials.²³ We

θ (deg)	S_{FM}	S_{AFM}	$E_{AFM} - E_{FM}$ (meV)	J (meV)
57	2.81	2.95	260	31
70	2.79	3.37	-456	-48
80	2.88	3.41	-645	-66
90	2.55	3.23	-415	-50
100	3.63	3.65	-170	-13
110	3.34	3.39	64	6

TABLE I: Magnetic characteristics of the $[HFeO]_2$ dimer calculated using the pseudopotential method for different Fe-O-Fe angles θ .

set the cutoff energies for the plane-wave expansion at 400 eV, and perform the calculation only for the Γ -point in the first Brillouin zone, which is sufficient for a single molecule calculation. To obtain the equilibrium structure of the dimer, we apply the optimization procedure that relaxes the system until the forces acting on each atom converge to within 0.02 eV/ \AA . We obtain the values S_{FM} and S_{AFM} for the local spins on the Fe sites in both the ferromagnetic and antiferromagnetic configurations by integrating the local spin densities over a sphere of radius 1.1 \AA centered about the Fe site. For each angle θ , the total energies E_{FM} and E_{AFM} for the antiferromagnetic and ferromagnetic configurations are calculated. Then, the exchange coupling J is determined from

$$J = \frac{E_{AFM} - E_{FM}}{S_{AFM} S_{FM}}. \quad (1)$$

Ideally, if the absolute energy values E_{FM} and E_{AFM} were reliable, we would calculate J from $E_{AFM}/S_{AFM}^2 - E_{FM}/S_{FM}^2$. We make the above approximation because the absolute energy values are not nearly as reliable as are the much smaller energy differences.

In order to find the equilibrium structure of the dimer, we first minimize the forces acting upon the atoms within the dimer. We find that the minimum energy is reached for antiferromagnetic states in which the Fe-O bond length $\ell = 1.83 \text{ \AA}$, and Fe-O-Fe bond angle $\theta = 82.4^\circ$. We then keep the bond length fixed to that optimum value, and calculate E_{FM} , E_{AFM} , S_{FM} , and S_{AFM} for six θ values in the range $57^\circ \leq \theta \leq 110^\circ$. Our results are presented in Table 1.

We find that for $\theta > 105^\circ$ and for $\theta < 63^\circ$, the dimer prefers to be in a ferromagnetic ground state, whereas for $63^\circ < \theta < 105^\circ$, an antiferromagnetic coupling is preferred. The change in magnetic order is accompanied by strong changes in the spin density on the Fe ions, as well as in the spin density on the O ions that control the superexchange interactions, which data are not presented. For the Fe dimer components in Fe8, the $[LFe(OH)]_2^{2+}$ effective dimers have $\theta = 100.7^\circ$, which our calculations indicate is likely to be antiferromagnetic, contrary to the experiments. The central effective $[LFeO]_2^{2+}$ dimer has $\theta = 104.4^\circ$, which is borderline between ferromagnetic

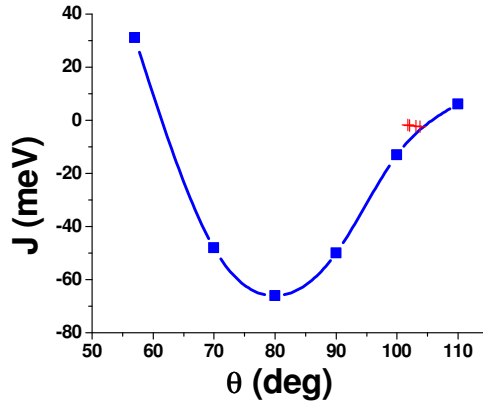


FIG. 2: Plot of the exchange energy J in meV versus the Fe-O-Fe angle θ in degrees. Shown are our results from Table 1 (solid blue square), a guide to the eye (solid blue curve), and the data for Fe2 dimers (red crosses).⁸

and antiferromagnetic in our calculations. Experimentally, it is ambiguous, because the ground state configuration of those spins are also affected by superexchange via a single oxygen in an OH^- ion, which is likely to be strongly antiferromagnetic.

In Fig. 2, we have plotted our $J(\theta)$ data, along with the experimental data of Le Gall *et al.* for the four Fe2 dimers.⁸ We note that the experimental data points are close to the guide to the eye between our calculated angles $\theta = 100, 100^\circ$, so that our pseudopotential calculation is close to predicting the experimentally observed exchange energies of these four compounds.

We remark that Pederson, Kortus, and Khanna have performed a much more accurate set of calculations for Fe8, and obtain the experimentally found S=10 ground state, with the central $[\text{LFeO}]_2^{2+}$ dimer being antiferromagnetically coupled to the other Fe spins.²⁴ They also found global anisotropy parameters in rather close agreement with experiment as deduced from magnetization experiments and from oscillations in the quantum tunnel splitting.^{25,26}

We note that although the dimer we have studied is rather different from the Fe2 dimers that exhibit superexchange via the oxygen ions in alkoxides, to the extent that the alkoxides can be approximated by the O^{2-} ions we studied, the θ values observed in the four Fe2 dimers varied from 101° to 104° , which are in the antiferromagnetic regime.⁸ As in the extended Hückel calculations, it appears that the general trend we calculate of increasing J with increasing θ is opposite to the experiments on the four Fe2 dimers. However, we do not have enough data points between 100° and 105° to determine if the general trend is accurately followed. More important, there appear to be serious discrepancies with the interesting case of $[\text{Fe(salen)}\text{Cl}]_2$, with $\theta \approx 90^\circ$ and a very weak, antiferromagnetic exchange interaction.^{15,16,17,18,20}

Fe d orbital	FM Fe1,2 \uparrow	FM Fe1,2 \downarrow	AFM Fe1 \uparrow	AFM Fe1 \downarrow	AFM Fe2 \uparrow	AFM Fe2 \downarrow
$d_{z^2-r^2}$	0.8454	0.2541	0.8451	0.2194	0.2192	0.8451
$d_{x^2-y^2}$	0.8822	0.4177	0.8875	0.0875	0.0885	0.8875
d_{xy}	0.8953	0.0549	0.8930	0.1321	0.1312	0.8931
d_{xz}	0.7494	0.2585	0.8777	0.3247	0.3247	0.8776
d_{yz}	0.8910	0.0562	0.8923	0.0921	0.0918	0.8923

TABLE II: FLAPW results for the partial charges within the Fe d -orbitals for $\theta = 100^\circ$. The FM and AFM cases for up and down spins within the Fe1 and Fe2 spheres are presented.

Fe d orbital	FM Fe1,2 \uparrow	FM Fe1,2 \downarrow	AFM Fe1 \uparrow	AFM Fe1 \downarrow	AFM Fe2 \uparrow	AFM Fe2 \downarrow
$d_{z^2-r^2}$	0.8407	0.2511	0.8431	0.2173	0.2172	0.8430
$d_{x^2-y^2}$	0.8830	0.4215	0.8911	0.0670	0.0669	0.8911
d_{xy}	0.8949	0.0613	0.8924	0.1490	0.1496	0.8924
d_{xz}	0.7555	0.2490	0.8849	0.3102	0.3102	0.8849
d_{yz}	0.8914	0.0533	0.8920	0.0936	0.0937	0.8920

TABLE III: FLAPW results for the partial charges within the Fe d -orbitals for $\theta = 105^\circ$. The FM and AFM cases for up and down spins within the Fe1 and Fe2 spheres are presented.

In addition, our pseudopotential calculation does not contain any specific information regarding the relative spin densities in the various occupied Fe orbitals. Hence, we are unable to determine the local spin anisotropy parameters relevant for more detailed studies of Fe2 dimers.¹³ In order to obtain useful information regarding the local spin anisotropies, another calculational procedure, such as a full potential augmented plane wave calculation, would be necessary. In $[\text{Fe}(\text{salen})\text{Cl}]_2$, the unusual behavior of the first magnetization step is strongly suggestive of a substantial local spin anisotropy interaction, as noted above.^{13,20}

As a preliminary check upon the validity of the pseudopotential method and also as a first-principles investigation of the possibility of local spin anisotropy, we have made full potential augmented plane wave (FLAPW) calculations of the spin densities and energies of the $[\text{HFeO}]_2$ dimer at $\theta = 100, 105^\circ$. In Tables II and III, we presented our results obtained using the FLAPW method for the partial charges in the various Fe(III) d -orbitals for both up (\uparrow) and down (\downarrow) spin configurations in the FM and AFM configurations, on Fe1 and Fe2 sites, for $\theta = 100, 105^\circ$, respectively. In Table IV, the energy differences between the FM and AFM cases for these angles are also presented.

In comparing our FLAPW results from Table IV with those obtained from the pseudopotential method in Table I, we see that they both predict a crossover from AFM behavior for $\theta \leq 100^\circ$ to FM behavior at larger angles. Although we did not perform the pseudopotential calculation at $\theta = 105^\circ$, our FLAPW calculation at 105° predicts FM behavior, so that the predicted crossover at

θ (deg)	$E_{AFM} - E_{FM}$ (eV)
100	-0.69134
105	1.0594

TABLE IV: FLAPW calculations of the energy differences between AFM and FM states for $\theta = 100, 105^\circ$

θ (deg)	FM Q_\uparrow	FM Q_\downarrow	AFM1 Q_\uparrow	AFM1 Q_\downarrow	AFM2 Q_\uparrow	AFM2 Q_\downarrow
100	8.49303	5.16213	8.63626	4.98165	4.98117	8.63650
105	8.49901	5.15439	8.64531	4.96278	4.96329	8.64520

TABLE V: Total charge densities on the Fe 1 and 2 sites for up and down spins, respectively, for the FM and AFM configurations, at the two angles studied using the FLAPW technique.

θ_c is for $100^\circ < \theta_c < 105^\circ$. In addition, it is evident that the largest differences in the spin densities at within the d_{xy} and d_{yz} orbitals for the FM case for both θ values, whereas comparable (for $\theta = 100^\circ$) or slightly larger (for $\theta = 105^\circ$) differences in the spin densities occur within the $d_{x^2-y^2}$ orbitals for the AFM configurations, respectively. We expect that the bonding orbitals will be the d_{xz} and $d_{z^2-r^2}$ orbitals, for which the magnitudes of the differences in the spin densities were found to be nearly equivalent for both the AFM and FM configurations, for

both angles studied. Thus, the spin density differences within the bonding orbitals, that participate in the exchange interactions, depend very weakly upon the Fe-O-Fe bond angle θ . The greatest θ dependence is for spin density differences in the non-bonding orbitals, and the orbital that shows the greatest distinction between FM and AFM behavior is the $d_{x^2-y^2}$ orbital. Thus, it appears that the $d_{x^2-y^2}$ -orbital governs the local spin anisotropy in Fe2 dimers.

In order to estimate the strength of the effective Heisenberg coupling, if we take the differences in the total spin densities from Table V, we obtain $J = -57$ meV and $J = 86$ meV for $\theta = 100, 105^\circ$, respectively. Taking the spins to have the value 4 in each case, we get $J = -43$ meV and $J = 66$ meV, respectively. These numbers are larger in magnitude than the values obtained using the pseudopotential technique.

We remark that the most interesting Fe2 dimer to date is [Fe(salen)Cl]₂, which has Cl ions in place of the H ions pictured in Fig. 1. In addition, there are organic ligands attached to the O ions, as in all of the Fe2 dimers presently known.^{8,15,20} We have not yet studied this very interesting case, but plan to do so soon. The Cl⁻ ions could polarize the local spins in the Fe *d*-orbitals, and it would be interesting to see if the $d_{z^2-r^2}$ orbitals would be the most affected.

This work was supported in part by the NSF through contract NER-0304665.

* Electronic address: stolbov@phys.ksu.edu

† Electronic address: klemm@phys.ksu.edu

‡ Electronic address: rahman@phys.ksu.edu

¹ R. Sessoli, D. Gatteschi, A. Caneschi, and M. A. Novak, Nature (London) **365**, 141 (1993).

² J. R. Friedman, M. D. Sarachik, J. Tejada, and R. Ziolo, Phys. Rev. Lett. **76**, 3830 (1996).

³ M. N. Neuenberger and D. Loss, Nature (London) **410**, 789 (2001).

⁴ W. Wernsdorfer, T. Ohm, C. Sangregorio, R. Sessoli, D. Mailly, and C. Paulsen, Phys. Rev. Lett. **82**, 3903 (1999).

⁵ D. Zipse, J. M. North, N. S. Dalal, S. Hill, and R. S. Edwards, Phys. Rev. B **68**, 184408 (2003).

⁶ K. Wieghardt, K. Phol, I. Jibril, and G. Huttner, Angew. Chem., Int. Ed. Engl. **23**, 77 (1984).

⁷ C. Sangregorio, T. Ohm, C. Paulsen, R. Sessoli, and D. Gatteschi, Phys. Rev. Lett. **78**, 4645 (1997).

⁸ F. Le Gall, F. Fabrizi de Biani, A. Caneschi, P. Cinelli, A. Cornia, A. C. Fabretti, and D. Gatteschi, Inorg. Chim. Acta **262**, 123 (1997).

⁹ A. Lascialfari, F. Tabak, G. L. Abbati, F. Borsa, M. Corti, and D. Gatteschi, J. Appl. Phys. **85**, 4539 (1999).

¹⁰ L. Cianchi, F. Del Giallo, M. Lantieri, P. Moretti, G. Spina, and A. Caneschi, Phys. Rev. B **69**, 014418 (2004).

¹¹ P. J. Hay, J. C. Thibeault, and R. Hoffman, J. Am. Chem. Soc. **97**, 4884 (1975).

¹² D. V. Efremov and R. A. Klemm, Phys. Rev. B **66**, 174427

(2002).

¹³ D. V. Efremov and R. A. Klemm, cond-mat/0409168.

¹⁴ M. Julve and O. Kahn, Inorg. Chim. Acta **76**, L39 (1983).

¹⁵ M. Gerlach and F. E. Mabbs, J. Chem. Soc. A **1967**, 1900.

¹⁶ M. Gerlach, J. Lewis, F. E. Mabbs, and A. Richards, J. Chem. Soc. A **1968**, 112.

¹⁷ W. M. Reiff, G. J. Lang, and W. A. Baker, Jr., J. Am. Chem. Soc. **90**, 6347 (1968).

¹⁸ R. Lechan, C. Nicolini, C. R. Abeledo, and R. B. Frankel, J. Chem. Phys. **59**, 3138 (1973).

¹⁹ Y. Shapira, M. T. Liu, S. Foner, R. J. Howard, and W. H. Armstrong, Phys. Rev. B **63**, 094422 (2001).

²⁰ Y. Shapira, M. T. Liu, S. Foner, C. E. Dubé, and P. J. Bonitatebus, Jr., Phys. Rev. B **59**, 1046 (1999).

²¹ J. P. Perdew and Y. Wang, Phys. Rev. B **45**, 13244 (1992).

²² M. C. Payne, M. P. Teter, D. C. Allen, T. A. Arias, and J. D. Joannopoulos, Rev. Mod. Phys. **64**, 1045 (1992).

²³ D. Vanderbilt, Phys. Rev. B **41**, 7892 (1990).

²⁴ M. R. Pederson, J. Kortus, and S. N. Khanna, J. Appl. Phys. **91**, 7149 (2002).

²⁵ R. Carciuffo, G. Amoretti, A. Murani, R. Sessoli, A. Caneschi, and D. Gatteschi, Phys. Rev. Lett. **81**, 4744 (1998).

²⁶ W. Wernsdorfer, R. Sessoli, A. Caneschi, D. Gatteschi, A. Cornia, and D. Mailly, J. Appl. Phys. **87**, 5481 (2000).